J. Serb. Chem. Soc. *65*(12)905–914(2000) UDC 621.352/.354:621.·˙316
JSCS–2818 *Original scientific paper*

A new current line division concept for the determination of the current distribution in electrochemical cells. Part I. Theoretical background of the "corner weakness" effect in electroforming

K. I. POPOV[1#] and R. M. STEVANOVIĆ [2#]

[1]*Faculty of Technology and Metallurgy, University of Belgrade, Karnegijeva 4, P. O. Box 35-03, YU-11001 Belgrade and* [2]*ICTM - Institute of Electrochemistry, Njegoševa 12, P. O. Box 815, YU-11001 Belgrade, Yugoslavia*

(Received 19 April, revised 28 August 2000)

A new approach to the determination of the current distribution in electrochemical cells, the current line division concept, is introduced. The new concept, based on the basic equations of electrics and electrochemical kinetics, was employed for a theoretical explanation of the phenomenon known in electroforming as "corner weakness". It was shown that this phenomenon depends on the kind of control of the deposition process, being the largest in the case of pure ohmic control and disappearing in the case of pure activation control.

Keywords: current distribution, current line division, electroforming, corner weakness.

INTRODUCTION

The problem of current distribution in electrochemical cells is regularly treated by employing fundamental equations of mass and charge transport.[1] Although particular cases permit certain simplifications, this approach requires rather complicated mathematical apparatus to obtain either analytical or numerical solutions of differential equations.

The purpose of this communication is to introduce another approach, which is more straightforward and easy to visualize, as it is based only on the Ohm and Kirchoff laws and basic equations of electrode kinetics. Tha validity of the new approach is demonstrated here by analysis of one typical example of uneven current distribution – the "corner weakness" phenomenon.

"Corner weakness" occurs in heavy deposits of electroforms at screened cathode parts *i.e.,* corners. At these areas, the deposit is thinner and, in extreme cases, there is no deposition at all along the line of corner bisector.[2,3] The consequence is the emergence of fracture under negligible load along the line of corner bisection, instead of fracture at

Serbian Chemical Society active member.

much higher loads across the narrowest cross-section of an electroform normal to the line of pull.

To the best of our knowledge, a theoretical analysis of this phenomenon has not been repored so far. The purpose of this work was to undertake one, using the following assumptions:

– the potential difference between each two points on the anode and cathode is equal to the cell voltage,

– the current lines are normal to the electrode surface,

– along each current line a corresponding ohmic resistance exists and the current lines are independent of and insulated from each other,

– current lines in the vicinity of a protrusion divide into components which are normal to the electrode surface and

– the Kirchoff laws are valid for current lines branching.

STATEMENT OF THE PROBLEM

Ohmic controlled deposition

The current distribution in a cell with the electrode arrangement given in Fig. 1 near to an elevation at the cathode can be envisaged as shown in Fig. 1b.

According to the assumed model of current line division it follows that there is no deposition along the line of bisection (from Fig. 1b). The current distribution in the cell

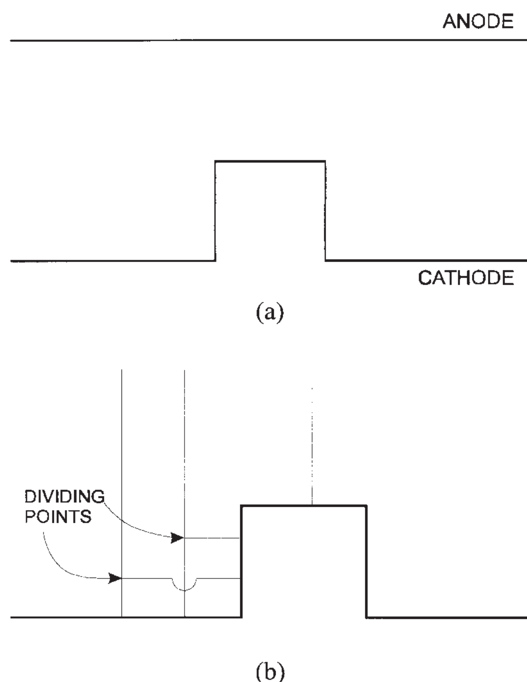

Fig. 1. a) Cathode with a protrusion in a cell with plane parallel electrodes. b) Current line division in the vicinity of the protrusion on the cathode.

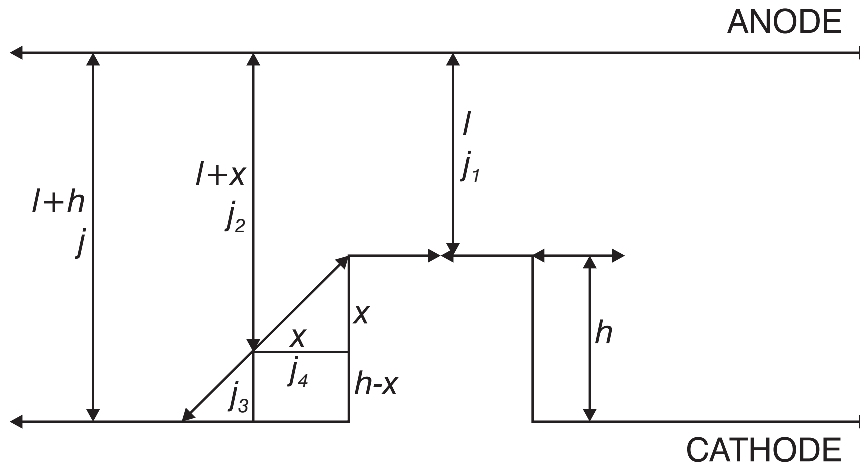

Fig. 2. Evaluation of the current distribution in the cell from Fig. 1a, using the concept of current line division from Fig. 1b.

from Fig. 1a is then given in Fig. 2, if current lines division takes place along the line indicated by the dashed line. It can be seen that this configuration provides the same density of current lines at the cathode as at the anode.

The ohmic potential drops along the current lines j and j_1 are given by Eqs (1) and (2), respectively.

$$E_{\text{cell}} = \rho(I + h)\,j \tag{1}$$

$$E_{\text{cell}} = \rho I j_1 \tag{2}$$

where E_{cell} is the cell voltage and ρ is the resistivity of the solution. The ohmic resistance along the current line j_2 is somewhat different. It consists of the resistance between the anode and the dividing point (DP) and two resistances connected in parallel between the DP and the cathode. Hence, the ohmic potential drop along current j_2 can be written as

$$E_{\text{cell}} = \rho j_2 \left[I + x + \frac{x(h-x)}{h} \right] \tag{3}$$

Elimination of E_{cell} from Eqs. (1) and (3) and further rearrangement gives

$$j(I+h) = j_2 \frac{hI + 2hx - x^2}{h} \tag{4}$$

It follows from Eq. (4) that for $x = h$

$$j_2 = j \tag{5}$$

and for $x = 0$

$$j_2 = j\frac{I+h}{I} = j_1 \tag{6}$$

Because it follows from Eqs. (1) and (2) that

$$j_1 = j\frac{l+h}{l} \tag{7}$$

The current densities j_3 and j_4 are given by

$$j_3 = \frac{\rho(l+h)j - \rho(l+x)j_2}{\rho(h-x)} \tag{8}$$

and

$$j_4 = \frac{\rho(l+h)j - \rho(l+x)j_2}{\rho x} \tag{9}$$

Substitution of j_2 from Eq. (4) into Eqs. (8) and (9) and further rearrangement gives

$$j_3 = \frac{E_{\text{cell}}}{\rho}\frac{x}{hl + 2hx - x^2} \tag{10}$$

and

$$j_4 = \frac{E_{\text{cell}}}{\rho}\frac{h-x}{hl + 2hx - x^2} \tag{11}$$

Now, by recalling Eq. (1), Eqs. (10) and (11) can be rewritten in the form, which enable the calculation of the deposit profiles at the cathodes represented by Figs. 1 and 2

$$j_3 = j\frac{(l+h)x}{hl + 2hx - x^2} \tag{12}$$

and

$$j_4 = j\frac{(l+h)(h-x)}{hl + 2hx - x^2} \tag{13}$$

Mixed activation – diffusion – ohmic controlled deposition

In this case, it is not possible to perform an analysis of the current density distribution in the same manner as in the case of ohmic controlled deposition. Only a numerical solution can be obtained, regardless of the fact that the current line distribution is the same as shown in Fig. 2.

In this case, the first step is the calculation of the voltage current curves, for interelectrode distances l and $l + h$, using Eqs. (14) and (15).

$$E_{\text{cell}} = \frac{b_{\text{a}}}{2.3}\ln\frac{j_1}{j_{0\text{a}}} + \frac{b_{\text{c}}}{2.3}\ln\frac{j}{j_{0\text{c}}}\frac{j_{\text{L}}}{j_{\text{L}} - j_1} + \rho l j_1 \tag{14}$$

$$E_{\text{cell}} = \frac{b_{\text{a}}}{2.3} \ln \frac{j}{j_{0\text{a}}} + \frac{b_{\text{c}}}{2.3} \ln \frac{j}{j_{0\text{c}}} \frac{j_{\text{L}}}{j_{\text{L}} - j} + \rho(I + h)j \tag{15}$$

where E_{cell} is the cell voltage, b_{a} and b_{c} and $j_{0\text{a}}$ and $j_{0\text{c}}$ are the anodic and cathodic Tafel slopes and exchange current densities, respectively, and j_{L} is the limiting diffusion current density for the cathodic process. Corresponding plots from Fig. 3 enable the determination of the current densities on the frontal parts of the cathode (j and j_1) for any cell voltage.

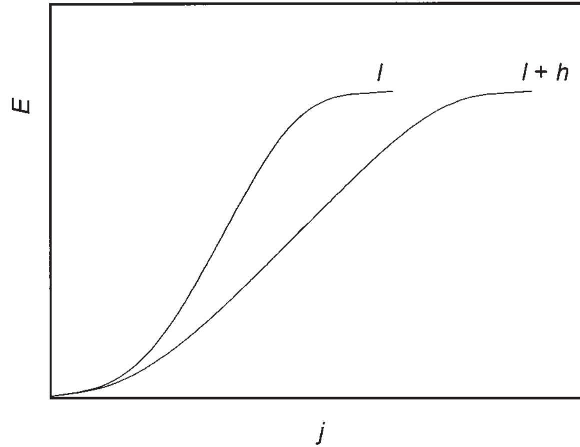

Fig. 3. Voltage current curves for interelectrode distances l and $l + h$.

The overall current density along the current line from the anode to the DP is obviously the sum of the partial ones branching at the DP, *i.e.*, $j_3 + j_4$. Hence, Eqs. (16) and (17) are valid

$$E_{\text{cell}} = \frac{b_{\text{a}}}{2.3} \ln \frac{j_3 + j_4}{j_{0\text{a}}} + \rho(I + x)(j_3 + j_4) + \frac{b_{\text{c}}}{2.3} \ln \frac{j_3}{j_{0\text{c}}} \frac{j_{\text{L}}}{j_{\text{L}} - j_3} + \rho j_3 (h - x) \tag{16}$$

$$E_{\text{cell}} = \frac{b_{\text{a}}}{2.3} \ln \frac{j_3 + j_4}{j_{0\text{a}}} + \rho(I + x)(j_3 + j_4) + \frac{b_{\text{c}}}{2.3} \ln \frac{j_4}{j_{0\text{c}}} \frac{j_{\text{L}}}{j_{\text{L}} - j_4} + \rho j_4 x \tag{17}$$

Elimination of E_{cell} from Eqs. (16) and (17) gives

$$\frac{b_{\text{c}}}{2.3} \ln \frac{j_3}{j_{0\text{c}}} \frac{j_{\text{L}}}{j_{\text{L}} - j_3} + \rho j_3 (h - x) = \frac{b_{\text{c}}}{2.3} \ln \frac{j_4}{j_{0\text{c}}} \frac{j_{\text{L}}}{j_{\text{L}} - j_4} + \rho j_4 x \tag{18}$$

Obviously, both sides of the Eq. (18) represent the potential drop between the DP and the cathode, E_{DPC}, which can be plotted as a function of either j_3 or j_4, as shown in Fig. 4a and Fig. 4b, respectively.

From the dependencies of Fig. 4, the corresponding values of j_3 and j_4 can be extracted by interpolation, for any E_{DPC} and x. These are required for the calculation of the potential drop between the anode and the DP, E_{ADP}, according to Eq. (19) and the overall cell voltage, E_{cell}, according to Eq. (20)

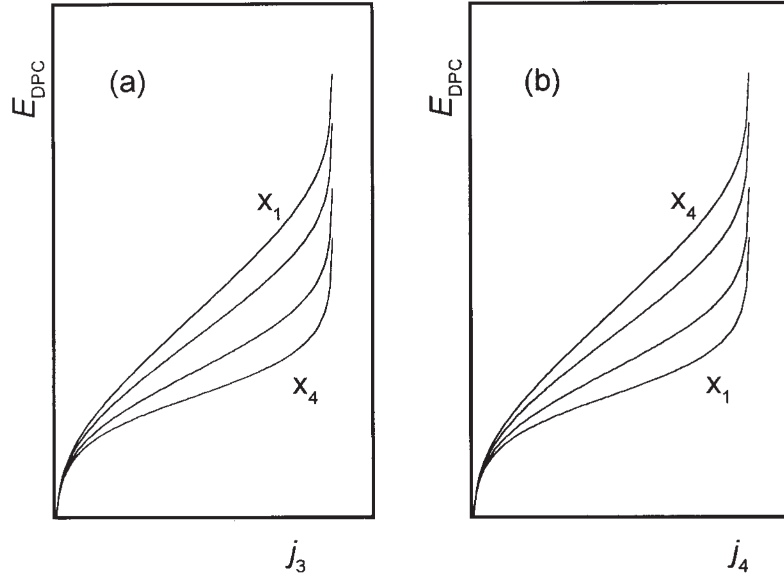

Fig. 4. Potential drop between the DP and the cathode, E_{DPC}, as a function of (a) j_3 and (b) j_4, for different values of x.

$$E_{ADP} = \frac{b_a}{2.3} \ln \frac{j_3 + j_4}{j_{0a}} + \rho(l + x)(j_3 + j_4) \tag{19}$$

$$E_{cell} = E_{ADP} + E_{DPC} \tag{20}$$

Now, E_{cell}, j_3 and j_4 can be tabulated or plotted as functions of the overall current density, $(j_3 + j_4)$, as exemplified in Fig. 5, for one value of x.

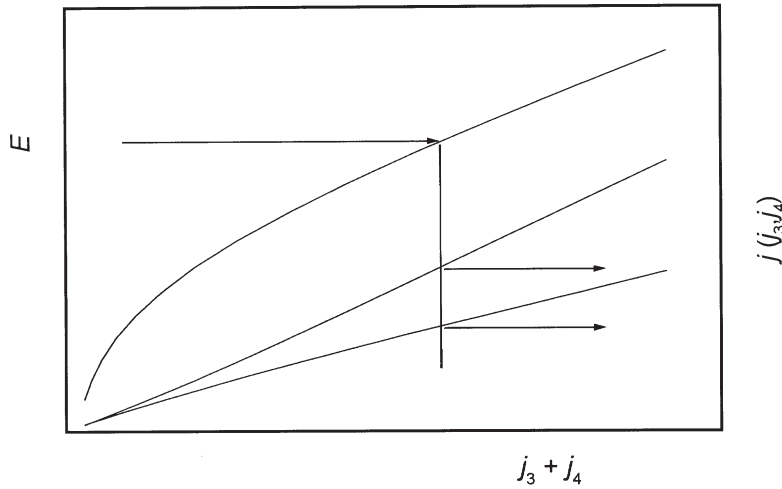

Fig. 5. Cell voltage E_{cell}, j_3 and j_4 as functions of the overall current $(j_3 + j_4)$ for one chosen value of x.

Finally, for a chosen (fixed) cell voltage, E_{cell}, the dependencies from Fig. 5 can be interpolated in order to obtain j_3 and j_4. The complete current distribution at the chosen cell voltage may be evaluated by repeating the interpolation for other values of x, *i.e.*, for points from the top of the protrusion down to the plain cathode surface.

Activation – diffusion controlled deposition

In this case, the current line between the DP and the cathode splits into two equal parts. Hence, for $j = j_3 = j_4$, one can write

$$E_{cell} = \frac{b_a}{2.3} \ln \frac{2j}{j_{0a}} + \frac{b_c}{2.3} \ln \frac{j_1}{j_{0c}} \frac{j_L}{j_L - j} \quad (21)$$

and at the same time

$$E_{cell} = \frac{b_a}{2.3} \ln \frac{j_1}{j_{0a}} + \frac{b_c}{2.3} \ln \frac{j_1}{j_{0c}} \frac{j_L}{j_L - j_1} \quad (22)$$

Elimintion of E_{cell} from Eqs. (21) and (22) permits the correlation between j and j_1 in the form of Eq. (23), which cannot be solved explicitly if $b_a \neq b_c$

$$b_a \ln \frac{2j}{j_1} = b_c \ln \frac{j_1}{j} \frac{j_L - j}{j_L - j_1} \quad (23)$$

If $j_L >> j$ and $j_L >> j_1$ Eq. (23) can be rewritten in the form

$$b_a \ln \frac{2j}{j_1} = b_c \ln \frac{j_1}{j} \quad (24)$$

or

$$j = j_1 2^{-\frac{b_a}{b_a + b_c}} \quad (25)$$

which holds for pure activation control.

DISCUSSION

The proposed model implies that there is no current component in the direction of the corner vertex, and that the appearance of a crack along the corner bisector is to be expected.

A compact deposit cannot be obtained directly, but rather by the build up of the deposit in the X and Y direction. An overlap of the X and Y oriented deposits should occur when current density virtually does not depend on the distance from the very corner. However, if the current density decreases upon approaching the corner vertex, the deposits would not overlap and a flaw would be created.

Equations (12) and (13) may be utilized for the calculation of the current density distribution at the beginning of deposition. The results of this calculation are shown in Fig. 6.

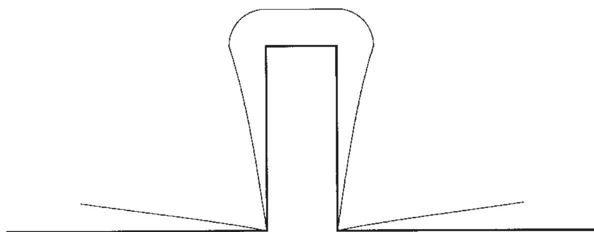

Fig. 6. Initial current profile at the model protrusion (h = 5 cm, l = 15 cm) calculated for pure ohmic control employing Eqs. (12) and (13).

Furher growth of the deposit is illustrated by Fig. 7. It is obvious that there should be no overlap of the deposit upon prolonged deposition. Moreover, it should be noted that the profiles were calculated assuming a constant current density, which is not the case in a real system where the space in the vicinity of the corner vertex is increasingly screened as the deposit grows. This implies that the real distribution of the metal deposit in the corners is worse than that calculated and shown in Fig. 7.

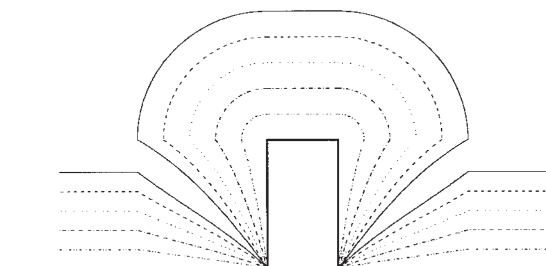

Fig. 7. Simulation of the growth of the deposit from Fig. 6.

A number of microphotographs of deposit cross-sections, illustrating the "corner weakness" effect, can be found in the literature.[2,3] They are schematically exemplified by Fig. 8. It can be seen that the calculated deposit profile (Fig. 7), with a crack appearing along the corner bisector, looks very similar to that typically obtained in plating practice (Fig. 8).

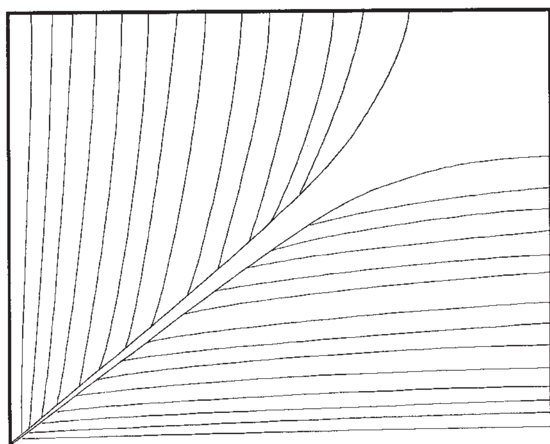

Fig. 8. Schematic representation of microphotographs[2,3] illustrating the "corner weakness" effect.

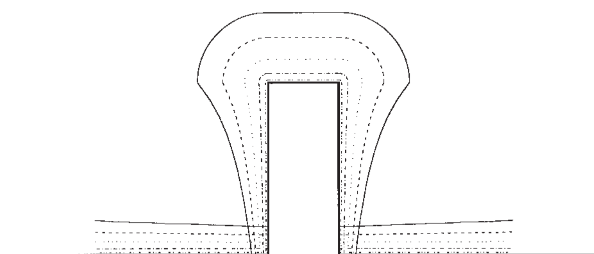

Fig. 9. Initial current profiles at the model protrusion ($h = 10$ cm, $l = 5$ cm) for mixed activation–diffusion–ohmic control, at E_{cell} ranging from 100 to 500 mV, calculated according to the procedure described by Eqs. (14) to (20).

The situation is similar in the case of mixed diffusion–activation control. The current density distribution (Fig. 9), as well as the profiles of the deposit at different times (Fig. 10 and Fig. 11) were calculated according to the procedures given above and the corresponding parameters: $j_0 = 0.05$ mA cm^{-2}; $j_L = 7$ mA cm^{-2}; $b_a = 40/2.3$ mV dec^{-1}; b_c=120/2.3 mV dec^{-1} and $\rho = 5\ \Omega$.

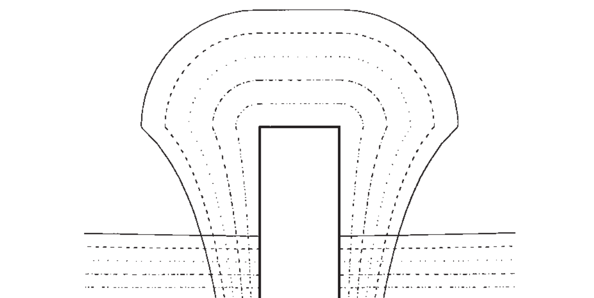

Fig. 10. Simulation of the further growth of the initial deposit obtained at E_{cell} of 300 mV (*cf.* Fig. 9).

Comparing the calculated deposit profiles for pure ohmic control (Fig. 6 and 7) with those pertaining to diffusion–activation control (Fig. 9 and 10), a significant difference in the cross section can be noticed. In the latter case, despite a much poorer system geometry (*cf.* h to l ratio) from the viewpoint of current distribution,[4] no failure in the deposit appears. Even so, a flaw in the deposit along the corner bisector may be expected in both cases.

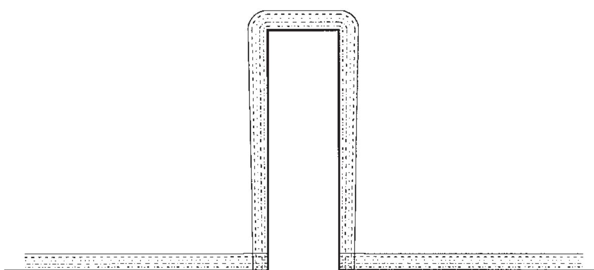

Fig. 11. Simulation of the further growth of the initial deposit obtained at a cell voltage of 100 mV (*cf.* Fig. 9).

Evenly distributed deposits, without "corner weakness", may be obtained only by deposition under complete activation control at high Tafel slopes (Fig. 11). In practice, this is usually achieved by employing appropriate surface-active additives, as seen in Fig. 12.[2,3]

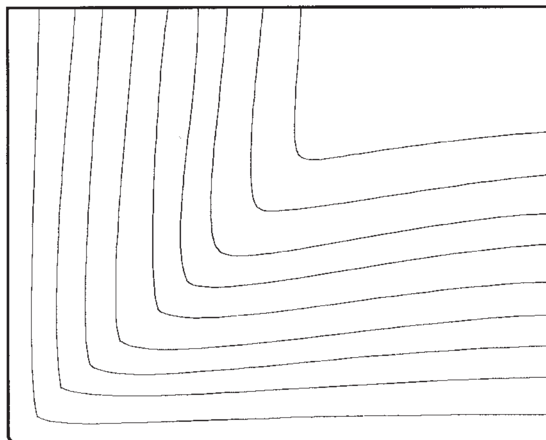

Fig. 12. Schematic representation of microphotographs of deposit cross-sections[2,3] illustrating the effect of surface active agents on the elimination of "corner weakness".

In this way not only is the "corner weakness" effect fully explained, but also a new method of current density distribution evaluation in electrochemical cells is promoted. An analysis of systems with geometries similar to that shown in Fig. 1, as well as the consideration of the importance of critical parameters, such as b_c, j_0, j_L, protrusion height to cell dimensions ratio (*h/l*), *etc.,* are to be the subject of forthcoming communications.

И З В О Д

НОВ КОНЦЕПТ ПОДЕЛЕ СТРУЈНИХ ЛИНИЈА ЗА ОДРЕЂИВАЊЕ РАСПОДЕЛЕ СТРУЈЕ У ЕЛЕКТРОХЕМИЈСКИМ ЋЕЛИЈАМА. ДЕО I. ТЕОРИЈСКЕ ОСНОВЕ ПОЈАВЕ "CORNER WEAKNESS" У ГАЛВАНОПЛАСТИЦИ

К. И. ПОПОВ[1] и Р. М. СТЕВАНОВИЋ[2]

[1]*Технолошко-металуршки факултет, Универзитет у Београду, Карнегијева 4, п. пр. 35-03, 11000 Београд и* [2]*ИХТМ - Центар за електрохемију, Његошева 12, п. пр. 815, 11001 Београд*

Предложен је нов приступ проблему одређивања расподеле струје у електрохемијским ћелијама, концепт поделе струјних линија. Концепт се базира на основним законима електротехнике и електрохемијске кинетике, и овде је употребљен за теоријско разматрање феномена који је у галванопластици познат као "corner weakness". Показано је да ова појава зависи од врсте контроле катодног процеса. Најизраженија је у условима чисте омске контроле, а изостаје у условима чисте активационе контроле.

(Примљено 19. априла, ревидирано 28. августа 2000)

REFERENCES

1. N. Ibl in *Comprenhensive Treatise of Electrochemistry*, E. Yeager, J. O'M. Bockris, B. E. Conway, S. Sarangapani, Eds., Vol 6, Ch. 5, Plenum Press, New York, 1983
2. Peter Spiro, *Electroforming*, Robert Drapper Ltd., Teddington, 1968, pp. 62
3. G. A. Sadakov, *Galvnoplastika*, Mashinostroienie, Moscow, 1987, pp. 17
4. K. I. Popov, R. M. Stevanović, this Journal, in preparation.